Optimization Design of Stabilizing Piles in Slopes Considering Spatial Variability

Wenping Gong[1], Huiming Tang[2], C. Hsein Juang[3], and Lei Wang[4]

[1] Professor, Faculty of Engineering, China University of Geosciences, Wuhan, Hubei 430074, China. Email: wenpinggong@cug.edu.cn
[2] Professor, Faculty of Engineering, China University of Geosciences, Wuhan, Hubei 430074, China. Email: tanghm@cug.edu.cn
[3] Chair Professor, Department of Civil Engineering and Graduate Institute of Applied Geology, National Central University, Taoyuan City 32001, Taiwan; also affiliate with Faculty of Engineering, China University of Geosciences, Wuhan, Hubei 430074, China, and Clemson University, Clemson SC 29634, USA. Email: hsein@clemson.edu
[4] Assistant Professor, Department of Civil Engineering, University of the District of Columbia, Washington, DC 20008, USA. Email: lei.wang@udc.edu (Corresponding author)

Abstract: Although advances in piling equipment and technologies have extended the global use of stabilizing piles (to stabilize slope or landslide), the design of stabilizing piles remains a challenge. Specifically, the installation of stabilizing piles can alter the behavior of the slope; and, the spatial variability of the geotechnical parameters required in the design is difficult to characterize with certainty, which can degrade the design performance. This paper presents an optimization-based design framework for stabilizing piles. The authors explicitly consider the coupling between the stabilizing piles and the slope, and the robustness of the stability of the reinforced slope against the spatial variability of the geotechnical parameters. The proposed design framework is implemented as a multi-objective optimization problem considering the design robustness as an objective, in addition to safety and cost efficiency, two objectives considered in the conventional design approaches. The design of stabilizing piles in an earth slope is studied as an example to illustrate the effectiveness of this new design framework. A comparison study is also undertaken to demonstrate the superiority of this new framework over the conventional design approaches.

Keywords: Stabilizing Piles; Slope; Factor of Safety; Design Robustness; Spatial Variability; Multi-Objective Optimization.

1. Introduction

"Stabilizing piles" are the piles that are installed to stabilize unstable slopes or active landslides, which transfer part of the earth pressure from the upper unstable layer to the lower stable layer, thus improving the stability of the geomaterials behind the piles (Poulos 1995; Zeng and Liang 2002; Lirer 2012). Since their inception, stabilizing piles have been widely used in the mitigation of slope instability and landslide geohazards. For example, many active landslides and unstable slopes in the Three Gorges Reservoir Area have been reinforced with stabilizing piles (Tang et al. 2014&2019). It is known that the installation of stabilizing piles can greatly alter the behavior of the slope. The stability of a reinforced slope could be evaluated with both uncoupled and coupled methods. In an uncoupled analysis, the earth pressure and its distribution along the piles are first estimated, followed by the use of the earth pressure as an input to the analysis of the behavior of the pile-slope system (Ito and Matsui 1975; Galli and Di Prisco 2012); whereas, in a coupled analysis, the piles and the slope are dealt as an integrated system, and the behavior of this system is studied considering explicitly the pile-slope interaction (Jeong et al. 2013). Though theoretically sound, the computationally demanding characteristics of this coupled analysis might hinder its application in engineering practice. As a result, the uncoupled analysis still dominates the design of stabilizing piles in the current practice.

Though the behavior of the pile-slope system has been the subject of extensive studies, little effort has been undertaken to elucidate design methods for stabilizing piles, especially on the selection of pile parameters such as the diameter, spacing, length and position (Lee et al. 1995). Indeed, the design of stabilizing piles is a multidisciplinary problem, which must be informed with knowledge of geotechnical engineering, structural engineering, and economics.

Hence, the design of the stabilizing piles would better be implemented as a multi-objective optimization problem, in which the requirements from the stability of the reinforced slope, bearing capacity of the piles, and economic concerns should be simultaneously considered. However, most of the discussions regarding the design of stabilizing piles do not encompass economic requirements but instead place most emphasis upon either the stability of reinforced slope or the pile bearing capacity (Chen and Martin 2002; Comodromos et al. 2009).

The geomaterials (e.g., soils and/or rocks) within a slope are natural materials, and the properties of the geomaterials are dependent upon the natural deposit and loading histories, which are beyond the control of the engineer. Due to the incomplete knowledge regarding the deposit and loading histories, the geotechnical properties at a site could not be known prior to the site investigation. In addition, because only a limited number of boreholes are afforded in a given project, the geotechnical properties are only known at the borehole locations. The properties at all other positions cannot be known and must be characterized from the known values at the borehole locations. Owing to the inherent spatial variability of the geotechnical properties and the limited availability of borehole data, the geotechnical properties at a given site will be uncertain. The uncertain geotechnical properties are often characterized with fuzzy or random variables, or random fields (Cho 2007; Wang et al. 2010; Ching and Phoon 2013; Tian et al. 2016; Xiao et al. 2016; Li et al. 2017; Wang et al. 2017; Xiao et al. 2017; Zhang et al. 2017; Liu and Cheng 2018; Kawa and Puła 2019; Tun et al. 2019). The uncertainty in the input geotechnical properties further complicates the design of stabilizing piles.

In the face of the geotechnical properties uncertainty, the level of stability of a slope, regardless of whether it is reinforced with stabilizing piles or not, will be uncertain and could not be expressed as a fixed value (Griffiths and Fenton 2004; Cho 2007; Li et al. 2016; Wang et al. 2018). To compensate for this uncertainty, a conservative estimate of the geotechnical properties is usually made in the design. And, to further ensure safety, the computed factor of safety *FS*, as a measure of the safety level, in a feasible design is required to be no less than a target *FS*. With such a deterministic design approach, however, the true safety of a candidate design is unknown, the resulting design might be either over- or under-designed. Alternatively, the probabilistic design approaches that allow for an explicit consideration of the uncertainty have long been advocated (Li and Lumb 1987; Christian et al. 1994; Duncan 2000; Juang et al. 2018). However, the designs obtained with the probabilistic approaches are strongly affected by the statistical information of the input geotechnical properties (Wang et al. 2013; Juang et al. 2014), which are difficult to characterize. Thus, the dilemma of whether to over-design for safety or under-design for cost efficiency has not been fully overcome, even though the design approaches evolve from deterministic to probabilistic approaches. To address this dilemma, robust design methods, originated in the field of quality and industrial engineering (Taguchi 1986; Phadke 1989; Beyer and Sendhoff 2007), have recently been adopted for applications in geotechnical designs (Juang and Wang 2013; Juang et al. 2014; Khoshnevisan et al. 2014). In the context of robust geotechnical design (RGD), the design robustness of the geotechnical system against the uncertainty in the input geotechnical parameters is explicitly considered along with cost and safety requirements.

In this paper, a new framework for the robust design of stabilizing piles is established that considers: 1) the coupling between the stabilizing piles and the slope; 2) the robustness of the stability of the reinforced slope against the uncertainty in the input parameters; and 3) the multi-objective optimization of the design robustness, economic aspect, and safety. The rest of this paper is organized as follows. First, this new optimization-based design framework for stabilizing piles is established. A hypothetical example, in terms of the design of stabilizing piles in a homogeneous earth slope, that utilizes this new design framework is then detailed. Thereafter, a comparison with the conventional geotechnical design approaches is undertaken to demonstrate the superiority of the advanced framework. Finally, the concluding remarks are made based upon the results presented.

2. New Design Framework for Stabilizing Piles in Slopes

While the significance of the coupling between the stabilizing piles and the slope, the uncertainty in the input geotechnical parameters, and the economic constraint in the design of stabilizing piles have long been recognized, an integrated design framework that can consider explicitly all these factors remains unavailable. In this paper, a new optimization-based design framework for stabilizing piles that considers all these factors simultaneously is advanced.

2.1 Modeling of the coupling in the pile-slope system

Figure 1 illustrates the coupling in a pile-slope system, in which the failure surface in an unreinforced slope and those in reinforced slopes (with three designs of stabilizing piles herein) are examined. In Figure 1(a), the depth of the failure surface in the unreinforced slope is shallow and passes above the slope toe. In Figure 1(b) and Figure 1(c), the piles are located around the middle part of the slope, and the pile lengths are greater than the depth of the initial failure surface; as a result, the failure surfaces in the reinforced slopes extend to greater depths. However, the length of the piles in Figure 1(b) is only slightly greater than the depth of the initial failure surface, unlike the one in Figure 1(c). Consequently, the failure surface in the reinforced slope in Figure 1(b) could not be blocked by the piles; and, the earth pressure transferred by the piles, indicated by the maximum bending moment of the piles M_{max}, is quite small (i.e., M_{max} = 99.4 kN·m), indicating that the bearing capacity of the piles cannot be fully utilized. On the other hand, the failure surface in the reinforced slope in Figure 1(c) could be blocked by the piles, and a greater part of the earth pressure from the upper unstable layer is transferred to the lower stable layer (i.e., M_{max} = 1153 kN·m). Thus, the improvement of the slope stability, indicated by the factor of safety of the reinforced slope FS_2, in Figure 1(c) is more significant (i.e., FS_2 = 1.28) than that in Figure 1(b) (i.e., FS_2 = 1.09). In Figure 1(d), the stabilizing piles are located in the lower part of the slope and the length of the piles is much greater than the depth of the initial failure surface, which causes a reduction in the length of the failure surface in the reinforced slope, and the new failure surface passes above the top of the piles. Note that although the earth pressure transferred by the piles is significant in Figure 1(d) (i.e., M_{max} = 1081 kN·m), the improvement of the slope stability is not apparent (i.e., FS_2 = 1.16). Thus, the failure surface, earth pressures on piles, and stability of reinforced slope are all affected by the coupling between the stabilizing piles and the slope. This coupling must be explicitly considered in the analysis and design of stabilizing piles.

Given the recognized effectiveness of numerical solutions for analyzing the coupling between the structures and the geomaterials, the 2-D explicit finite difference program FLAC version 7.0 (2011) is adopted herein as the solution model for evaluating the stability of the pile-slope system. Within FLAC version 7.0, the slope stability is evaluated with the strength reduction method, in which the resistance (i.e., shear strength) of the geomaterials is gradually adjusted to bring the slope (either reinforced or unreinforced) to the limit equilibrium state. It is well known that the behavior of a pile-slope system is a 3-D problem and which should be studied with 3-D numerical simulations; otherwise, the sliding of the geomaterials through the space between adjacent piles could not be simulated. However, the 3-D numerical simulation can be computationally prohibitive for the following probabilistic stability analysis and design optimization. In reference to Kourkoulis et al. (2010), an effective soil arching can be formed between adjacent piles when the ratio of the pile spacing over the pile diameter is less than 4.0. Under such circumstances, the plane-strain condition is taken in this study and the maximum ratio of the pile spacing (i.e., center-to-center spacing between piles) over the pile diameter is set to be 3.0. Thus, the stability of the pile-slope system can be evaluated with 2-D numerical simulations; in which, the piles are modeled with elastic-perfectly plastic beam elements, the interfaces between the piles and the geomaterials are modeled with interface elements, and the pile spacing is inputted to the numerical models to realize the resistance of the piles (against slope failure) per longitudinal length. The plastic moment of the piles, which is required in the 2-D numerical simulations, is derived with plasticity theory of reinforced concrete. Since the stability of a slope (either reinforced or unreinforced) can be dominated by the shear strength of the geomaterials, the behaviors of the geomaterials in this study are simulated with Mohr-Coulomb models.

2.2 Formulation of the design robustness of the reinforced slope

For the pile-slope system with the design parameters $\boldsymbol{d}$ and the non-design variables $\boldsymbol{\theta}$ as inputs, the response or performance of this system $g(\boldsymbol{d}, \boldsymbol{\theta})$ is expressed as:

$$g(\boldsymbol{d},\boldsymbol{\theta}) = R(\boldsymbol{d},\boldsymbol{\theta}) - T(\boldsymbol{d},\boldsymbol{\theta}) \tag{1}$$

where $R(\boldsymbol{d}, \boldsymbol{\theta})$ and $T(\boldsymbol{d}, \boldsymbol{\theta})$ are the resistance term and load term, respectively. Mathematically, the uncertainty in the input parameters $\boldsymbol{\theta}$ will lead to the uncertainty in the output or system response $g(\boldsymbol{d}, \boldsymbol{\theta})$. In reference to Figure 2, the relationship between the output $g(\boldsymbol{d}, \boldsymbol{\theta})$ and the inputs $\boldsymbol{\theta}$ is captured by a monotonic performance function $g(\boldsymbol{d}, \boldsymbol{\theta})$. For an arbitrary distribution of the inputs $\boldsymbol{\theta}$, the output $g(\boldsymbol{d}, \boldsymbol{\theta})$ is a distribution, rather than a fixed value.

In a deterministic design, the safety of a design is evaluated and expressed as a factor of safety *FS*:

$$FS = \frac{R(\boldsymbol{d},\boldsymbol{\theta})}{T(\boldsymbol{d},\boldsymbol{\theta})} \tag{2}$$

In practice, a design is deemed feasible if the computed *FS* is greater than 1.0. To compensate for the uncertainty in the input parameters and adopted model, a conservative estimate of the input parameters (e.g., 20^{th} percentile of the resistance term *R* and 80^{th} percentile of the load term *T*; see Figure 2) and a target *FS*, FS_T (e.g., FS_T = a value greater than 1.0, say, 1.2), may be adopted. Since the uncertainty is not explicitly included in the analysis, the true safety of the design is unknown and the resulting design might be either over- or under-designed. To overcome this problem, the probabilistic approaches which permit an explicit consideration of the uncertainty (e.g., uncertain variables are simulated as random variables or random fields) have long been advocated (Li and Lumb 1987; Christian et al. 1994; Cherubini 2000; Duncan 2000). In probabilistic designs, the safety of a design $\boldsymbol{d}$ is evaluated with the computed failure probability P_f or reliability index β.

$$P_f = \Pr[g(\boldsymbol{d},\boldsymbol{\theta}) < 0] = \int_{g(\boldsymbol{d},\boldsymbol{\theta})<0} f(\boldsymbol{\theta})d\boldsymbol{\theta} = \int_{-\infty}^{0} f(g)dg \tag{3a}$$

$$P_f = \Phi(-\beta) \tag{3b}$$

where $f(\boldsymbol{\theta})$ is the probability density function (PDF) of the uncertain input parameters $\boldsymbol{\theta}$; $f(g)$ is the PDF of the performance function $g(\boldsymbol{d}, \boldsymbol{\theta})$; and, $\Phi(\cdot)$ is the cumulative distribution function (CDF) of the standard normal variable. To ensure the safety of the resulting design, a target failure probability P_{fT} (e.g., $P_{fT} = 4.7\times10^{-3}$) or a target reliability index β_T (e.g., $\beta_T = 2.6$) is suggested. A design is deemed feasible if the computed failure probability P_f is less than the target failure probability P_{fT} or the related reliability index β is larger than the target reliability index β_T.

Note that while the formulation is simple and easy-to-follow, the practical application of the probabilistic approaches in the geotechnical design is not an easy task. The challenge in the geotechnical design is attributed to the fact that the geomaterials are natural, rather than manufactured materials. The degree of uncertainty in the geotechnical properties tends to be greater than that in the structural counterpart and the uncertainty in the geotechnical properties could be much more difficult to characterize. Furthermore, the property of the geomaterials is often spatially correlated. The spatial correlation characteristics of the geotechnical properties could best be characterized with the random field theory (Fenton 1999; Cho 2007; Tian et al. 2016). The anisotropic exponential autocorrelation structure is adopted herein to capture the spatial correlation of the geotechnical properties:

$$\rho\left(\left|x_1-x_2\right|,\left|y_1-y_2\right|\right)=\exp\left(-\frac{2\left|x_1-x_2\right|}{\lambda_{\mathrm{h}}}\right)\exp\left(-\frac{2\left|y_1-y_2\right|}{\lambda_{\mathrm{v}}}\right) \tag{4}$$

where $|x_1 - x_2|$ is the horizontal distance between the two positions of (x_1, y_1) and (x_2, y_2); $|y_1 - y_2|$ is the vertical distance between the two positions of (x_1, y_1) and (x_2, y_2); and, λ_{h} and λ_{v} are the horizontal and vertical scale of fluctuations of the geotechnical properties, respectively.

In a numerical modeling of a slope (either reinforced or unreinforced), the geometrical domain of the slope is discretized into a set of small elements, thus permitting an assignment of different geotechnical properties to different numerical elements. That is to say, the spatial variability of the geotechnical parameters can be directly simulated in the numerical modeling. Note that while lots of computationally efficient methods have been developed for the probabilistic analysis of the geotechnical systems, most of them cannot be applied to geotechnical systems with random fields as inputs; whereas, the sampling-based methods such as the Monte Carlo simulation (MCS) are often deemed the most reliable approaches for dealing with the random fields. To consider the spatial variability of the input geotechnical parameters in the design of stabilizing piles, the random finite difference method (RFDM) is adopted in this study. In the context of the RFDM, the spatial variability of the input geotechnical parameters is simulated with the random field theory, and potential realizations of the random field of the geotechnical parameters are sampled with MCSs. For each and every realization of the random field, the stability of the slope will be analyzed deterministically utilizing the finite difference program (e.g., the 2-D FLAC adopted in this paper). Since the parameters within a numerical element are captured by fixed parameters and no variation can be allowed, the geotechnical parameters that are averaged within the element domain, rather than those at the grids, should be sampled and taken as the inputs to the numerical analysis. The integration of brute MCS and numerical analysis can be computationally prohibitive. To improve the computational efficiency (of this RFDM), the subdomain sampling method (SSM) (Juang et al. 2017), in lieu of the brute MCS, is adopted in this paper for sampling the potential realizations of the random field of the input geotechnical parameters. A detailed formulation of this SSM is summarized in Appendix A.

In a typical geotechnical practice, site-specific data can be quite limited due to budget constraints for site investigation. Thus, it is difficult to derive the statistical information of the input geotechnical parameters with certainty (Gong et al. 2017). In such a circumstance, the probabilistic approaches are usually undertaken using inaccurate or assumed statistics; however, the designs obtained with the probabilistic approaches are strongly influenced by the adopted statistics (Wang et al. 2013). To overcome this issue of the probabilistic approaches, robust design, originated from the field of quality and industrial engineering (Taguchi 1986), is adopted, in this paper, for the design of stabilizing piles. The essence of this robust design is to derive a design in which the system behavior is robust against the uncertainty in the input parameters. In the proposed robust design of stabilizing piles, the robustness of the stability of the reinforced slope against the uncertainty (i.e., spatial variability) in the input geotechnical parameters, R, is formulated based upon the concept of "signal-to-noise ratio" (SNR) (Phadke 1989; Gong et al. 2014a).

$$R = SNR = 10 \log_{10}\left(\frac{E^2[FS_2]}{\sigma^2[FS_2]}\right) \tag{5}$$

where $E[FS_2]$ and $\sigma[FS_2]$ are the mean and standard deviation, respectively, of the stability of the reinforced slope. Note that although various robustness measures have been developed for the robust geotechnical design (RGD) (Wang et al. 2013; Juang et al. 2014; Khoshnevisan et al. 2014; Gong et al. 2014a&2014b), the selection of the robustness measure can be problem-specific depending upon the level of uncertainty in geotechnical parameters characterization: 1) in the scenario where only the nominal values of the geotechnical parameters are known, the gradient-based robustness may be utilized (Gong et al. 2014b); 2) in the scenario where the ranges of the geotechnical parameters could be estimated, the SNR-based robustness may be utilized (Gong et al. 2014a); and 3) in the scenario where the probabilistic distribution of the geotechnical parameters may be characterized but the statistical information could not be ascertained, the feasibility-based robustness may be used (Wang et al. 2013). In the proposed robust design of stabilizing piles, the *noise factors* (i.e., difficult-to-characterize and hard-to-control parameters) are *mainly* associated with the spatially varied geotechnical parameters. Note that while the feasibility-based robustness is theoretically sound, the simpler SNR-based robustness measure formulated in Eq. (5) is adopted herein owing to its simplicity and practical applicability. As such, the calculation of the feasibility of the failure probability satisfying the target failure probability can be avoided; meanwhile, the characterization of the *uncertainty in the statistical parameters* of the geotechnical properties, which is required for the feasibility calculation, can be avoided.

With the numerical model established in the previous section as a solution model, the uncertainty in the noise factors naturally propagates into the uncertainty in the stability of the reinforced slope, which could be captured by the standard deviation of the stability (in terms of the factor of safety FS) of the reinforced slope $\sigma[FS_2]$. It is noted that a higher $\sigma[FS_2]$ value indicates a higher variability of the stability of the reinforced slope (in the face of the input geotechnical properties uncertainty), thus signaling a lower robustness of the stabilizing pile design. Since the safety of the stabilizing pile design can also be affected by the mean of the stability of the reinforced slope $E[FS_2]$, the standard deviation of the stability $\sigma[FS_2]$ is further normalized by the mean of the stability $E[FS_2]$. Then, the SNR-based robustness R is readily formulated, as shown in Eq. (5). Similarly, a higher R value signals a lower variability of the stability of the reinforced slope, and thus indicating a higher robustness. Here, the detailed procedure for derivation of the mean $E[FS_2]$ and standard deviation $\sigma[FS_2]$ of the stability of the reinforced slope using the subdomain sampling method (SSM) is given in Appendix A. In reference to the robustness measure formulated in Eq. (5), the conventional factor of safety FS is embedded in this design robustness; and, this design robustness measure is calculated from the by-products of the probabilistic analysis, in terms of the statistics of the factor of safety FS. Hence, the proposed design framework is compatible with the conventional deterministic and probabilistic design approaches; and, the computational coupling of the evaluation of the design robustness and the probabilistic analysis would not lead to significant increase in the computational demands of the advanced robust design. Indeed, the only increase in the computational demand of the advanced design framework is the multi-optimization shown in Eq. (6), in comparison to the conventional probabilistic design approaches.

2.3 Optimization-based design of stabilizing piles incorporating robustness

The goal of the advanced optimization-based design framework for stabilizing piles is to derive an optimal stabilizing pile design (represented by a set of design parameters ***d***) in the design space ***DS*** such that the target stability of the reinforced slope ***TS*** can be satisfied, while both robustness *R* and cost efficiency *E* will be simultaneously optimized. This optimization-based design framework for stabilizing piles is set up as follows.

$$\begin{array}{ll} \text{Find:} & \text{Pile parameters } \boldsymbol{d} \\ \text{Subject to:} & \text{Design space } \boldsymbol{DS} \\ & \text{Target stability of reinforced slope } \boldsymbol{TS} \\ & \text{Ultimate bearing capacity of stabilizing piles } M_{\text{ult}} \\ \text{Objectives:} & \text{Maximizing design robustness } R \\ & \text{Minimizing construction cost } C \end{array} \quad (6)$$

where ***d*** represents the design parameters of the stabilizing piles that are easy-to-control (by the engineer). For example, the geometrical parameters of the pile diameter *D*, pile spacing *S*, pile length *L* and pile position *X* are taken as the design parameters ***d***, expressed as ***d*** = {*D*, *S*, *L*, *X*}. Whereas, the mechanical parameters of the piles such as the steel reinforcement ratio and concrete modulus are taken as fixed values; and, the steel strength and concrete strength, which are essential for estimating the ultimate bearing capacity of the piles, could be dealt as uncertain parameters (or noise factors) due to the manufacturing error.

The design space ***DS*** is an assembly of candidate designs of stabilizing piles, which can be determined based upon local experience and engineering judgment. The target stability

TS is a mandatory requirement of the stability of the reinforced slope, expressed in terms of the target factor of safety FS_T or target failure probability P_{fT} (or equivalently target reliability index β_T), which could be specified by the owner or client based upon the significance of the project or consequences of failure. The ultimate bearing capacity M_{ult} is the plastic moment of the piles, which is evaluated with the plasticity theory of steel reinforced concrete. The design robustness R is the "signal-to-noise ratio" (SNR) of the stability of the reinforced slope against the variation in the uncertain input parameters (or noise factors). The construction cost C is the economic aspect of the design of stabilizing piles. Assuming no variation in the cost with respect to the site condition and pile installation technique in a given project, only the material cost of the piles is considered in this paper. Further, the steel reinforcement ratio of the piles is taken as a fixed value. Thus, the cost C could be approximated herein by the volume of the stabilizing piles per longitudinal length.

$$C = \frac{\pi \cdot D^2 \cdot L}{4S} C_0 \tag{7}$$

where C_0 represents the cost per cubic meter of steel reinforcement concrete.

The desire to maximize the design robustness R and that to minimize the cost C are two conflicting objectives. The optimization in Eq. (6) cannot lead to a single best design with respect to both objectives simultaneously. Instead, this optimization only leads to a set of non-dominated designs which are superior to all others in the design space, but not superior or inferior to any other in this set. As depicted in Figure 3, although the non-dominated design $\boldsymbol{d}_1$ is less expensive (indicating higher cost efficiency), the counterpart of non-dominated design $\boldsymbol{d}_2$ yields a larger R value (indicating higher robustness). Note that although the utopia design $\boldsymbol{d}_0$ is optimal with respect to both objectives, it may not be located in the feasible domain (i.e., the target stability ***TS*** is not satisfied or not belong to design space ***DS***). These non-dominated designs collectively form a Pareto front which reveals a tradeoff relationship between these two conflicting design objectives (Deb et al. 2002; Juang et al. 2014). This Pareto front can be obtained utilizing multi-objective optimization algorithms such as the Multi-objective Genetic Algorithm, MOGA (Murata and Ishibuchi 1995), Niched Pareto Genetic Algorithm, NPGA (Horn et al. 1994), Non-dominated Sorting Genetic Algorithm version II, NSGA-II (Deb et al. 2002; Juang and Wang 2013), Multi-algorithm Genetically Adaptive Multiobjective Method, AMALGAM (Vrugt and Robinson 2007; Huang et al. 2014), weighted sum-based algorithm (Hajela and Lin 1992), or spreadsheet-based algorithm (Khoshnevisan et al. 2014).

Note that although various optimization algorithms could be available in the literature of industrial, civil and electrical engineering, the optimization of the geotechnical system such as the stabilizing piles is different from the optimization problem in other fields. For example, the choice of the pile diameter is limited to piling equipment and local practice, only discrete values can be taken. A survey of the geometrical parameters of the stabilizing piles installed in the Three Gorges Reservoir Area, China indicates that the pile lengths were often taken as discrete or integer values and the piles were usually constructed at the elevations of discrete or integer values. Thus, a discrete design space ***DS*** is selected in this paper for the optimization design of stabilizing piles to ensure the feasibility in the construction. Since a discrete design space is adopted with a finite number of candidate designs (e.g., 480 designs in this paper), the optimization presented in this study adopts an exhaustive search among the designs in the discrete design space, which is different from many other optimization techniques reported in the literature (e.g., Hajela and Lin 1992; Murata and Ishibuchi 1995; Deb et al. 2002; Vrugt and Robinson 2007), where potential candidate designs are generated and analyzed selectively, and not exhaustively. Here, the safety, robustness, and cost for each and every candidate design in the selected discrete design space are evaluated. On the basis of the evaluated performance of candidate designs, the Pareto front revealing the tradeoff between design robustness and cost efficiency can be derived utilizing the non-dominated sorting algorithm in the NSGA-II (Deb et al. 2002). It should be noted that although a discrete design space is adopted in this study, it is not the limitation of the advanced design framework and a continuous design space can also be adopted if so desired (and then the optimization algorithms reported in the literature can be applied); however, the random finite difference method (RFDM)-based probabilistic analysis of the candidate design will be iteratively called in the direct application of these optimization algorithms, which might increase the computational efforts for this problem.

The obtained Pareto front could help render an informed design decision. For example, either the least cost design that is above a pre-specified level of robustness R_P (see design $\boldsymbol{d}_3$ in Figure 3) or the most robust design that is below a pre-specified level of cost C_P (see design $\boldsymbol{d}_4$ in Figure 3) can be selected as the most preferred design in the design space ***DS***. However, the determination of an appropriate level of the robustness or cost is usually problem-specific. In situations where a strong preference is not pre-specified by the owner or client, the knee point on the Pareto front, which can yield the best compromise with respect to the conflicting objectives, can be identified (see design $\boldsymbol{d}_5$ in Figure 3) and taken as the most preferred design (Deb and Gupta 2011). As illustrated in Figure 3, on the left side of the knee point design $\boldsymbol{d}_5$, a slight reduction in cost C could lead to a drastic decrease in the design robustness R, which is not desirable; and, on the right side of the knee point design $\boldsymbol{d}_5$, a slight improvement in the design robustness R requires a huge increase in cost C, which is also not desirable. Thus, this knee point design could be taken as the most preferred design in the design pool, if no design preference is specified by the owner or client. Once the Pareto front is obtained, this knee point design is easily identified with the marginal utility function approach (Deb and Gupta 2011), normal boundary intersection approach (Deb and Gupta 2011), reflex angle approach (Deb and Gupta 2011), or minimum distance approach (Gong et al. 2016a).

As can be seen, the coupling between the stabilizing piles and the slope, the robustness of the stability of the reinforced slope against the uncertainty in the input parameters (e.g., the spatial variability of the geotechnical parameters and the manufacturing error of the structural materials), economic aspect, and conventional safety requirements are explicitly considered in the advanced design framework for stabilizing piles; and, this design framework is carried out through a multi-objective optimization with respect to these design objectives.

3. Illustrative Example: Design of Stabilizing Piles in An Earth Slope

To demonstrate the effectiveness and significance of the advanced design framework, the design of stabilizing piles in a homogeneous earth slope, shown in Figure 4, is adopted as an illustrative example. The parameters setting and the design results are presented below.

3.1 Parameters setting in the illustrative example

In reference to Figure 4, the width and height of the studied slope are 20.0 m and 14.0 m, respectively, and the depth to bed rock is assumed to approach infinity ($H \rightarrow \infty$). Further assume no surcharge on the top of the slope and the groundwater level far below the slope. In this example, both soil strength parameters, in terms of the cohesion c and friction angle ϕ, are treated as random fields, and their statistical information is tabulated in Table 1. The other soil parameters such as the unit weight, bulk modulus and shear modulus are assumed as fixed (or deterministic) values, as listed in Table 2.

An initial analysis of this slope indicates that the stability of this slope is relatively low (i.e., $FS_1 = 1.14$), which is thus designed to be reinforced by a single row of steel reinforced concrete stabilizing piles. According to the optimization framework outlined above, the easy-to-control geometrical parameters, including the pile diameter D, pile spacing S, pile length L and pile position X, are taken as the design parameters $\boldsymbol{d}$, expressed as $\boldsymbol{d} = \{D, S, L, X\}$. The steel reinforcement ratio and concrete modulus (of the piles) are treated as fixed values, as shown in Table 2; and, the steel strength and concrete strength are taken as uncertain input parameters and their statistical information is also given in Table 1. For ease of construction, a discrete design space ***DS*** shown in Table 3 is selected in this paper for the optimization design. The maximum ratio of the pile spacing S over the pile diameter D is set to be 3.0 (i.e., S/D = 3.0) in this optimization problem, thus effective soil arching can be formed between adjacent piles (Kourkoulis et al. 2010). In the selected design space ***DS*** shown in Table 3, a total of 480 candidate designs are possible and the optimal design will be identified from this pool.

To incorporate the coupling between the stabilizing piles and the slope explicitly, the numerical model established above is adopted herein as the solution model for evaluating the safety performance of the pile-slope system. The 2-D explicit finite difference program FLAC version 7.0 (2011) is used and plane-strain condition is assumed. To minimize the boundary effect, the bottom boundary is set at 30.0 m below the slope toe, the left-side boundary is set at 30.0 m away from the slope toe, and the right-side boundary is set at 30.0 m away from the slope crest. The geometrical domain of this slope problem is discretized into 1,296 elements (the minimum size of the discretized elements is 1.0 m×1.0 m) for ease of assigning the soil parameters (e.g., c and ϕ). The left- and right-side boundaries are restrained horizontally, and the bottom boundary is restrained vertically. The soil is simulated with Mohr-Coulomb model, the stabilizing piles are modeled with elastic-perfectly plastic beam elements, and the soil-pile interfaces are modeled with interface elements. The setting of the parameters of the piles and those of the interfaces is tabulated in Table 2. Note that a bracketing approach similar to that proposed by Dawson et al (1999) is used in FLAC version 7 for deriving the factor of safety *FS* of the slope, and the resolution limit is set at 0.02 in this paper. As such, the model error of this numerical model, in terms of the discrepancy between the true *FS* and the calculated *FS* (i.e., true *FS* minus calculated *FS*), might be taken as an uncertain variable that is uniformly distributed in the range of [-0.02, 0.02].

It should be noted that the execution of a deterministic analysis of the slope stability takes about 100 seconds on the Windows 7® PC equipped with a 192 GB RAM and an Intel® Xeon® Processor E5-2699 v4 @ 2.20 GHz. To reduce the number of the realizations or samples of the uncertain input parameters involved in the RFDM analysis and thus improving the computational efficiency, the subdomain sampling method (SSM) (Juang et al. 2017) is utilized for generating the realizations of the random fields of soil strength parameters and the samples of the other uncertain parameters (i.e., the steel strength, concrete strength and model error). The parameters of the adopted SSM are set up as follows: 1) the probability of ε in Eq. (A3) is taken as $\varepsilon = 1.0\times10^{-6}$ for locating the possible domain of uncertain parameters; 2) the likelihoods of the samples being located in the subdomains are taken as a decreasing sequence of $p_{d1} = 1/3$, $p_{d2} = 1/3^2$, $p_{d3} = 1/3^3$, … ; 3) the target number of samples in each subdomain is taken as $t_1 = 30$; and 4) the number of subdomains is taken as $n_s = 13$. Thus, a total of 390 realizations or samples of the uncertain input parameters will be generated and analyzed for estimating the statistics of the stability of the slope (either reinforced or unreinforced). This number of samples is close to that required in the stochastic response surface method (Li et al. 2011&2015), which is well known for its high computational efficiency in analyzing random field problems.

3.2 Results obtained with the advanced optimization-based design framework

With the derived statistics of the stability of the reinforced slope (using SSM), the design robustness R, in terms of the "signal-to-noise ratio" (SNR), and the design safety, in terms of the mean of the stability $E[FS_2]$ (to be compatible with the deterministic approach) or failure probability P_f (to be compatible with the probabilistic approach) of the reinforced slope, can readily be evaluated. For example, the failure probability of the reinforced slope P_f (or equivalent reliability index β) in this paper is estimated with the fourth moment method FM-1 outlined in Zhao and Ono (2001). Figure 5 validates the effectiveness and accuracy of the adopted SSM, using MCS, in deriving the design robustness R, design safety $E[FS_2]$ and design safety P_f of the reinforced slope through an analysis of 15 arbitrarily selected candidate designs. Note that the number of samples utilized in the brute MCS herein is taken as 5,000. In Figure 5(a) and Figure 5(b), the data points (of design robustness R and safety $E[FS_2]$) are both close to the 1:1 line (i.e., a perfect match), thus the design robustness R and design safety $E[FS_2]$ estimated from the adopted SSM match well with those from the MCS. In Figure 5(c), although there is some discrepancy in the derived failure probability P_f between the SSM and the MCS, the 90% confidence interval of the failure probability P_f derived from the MCS can bracket the failure probability P_f derived from the SSM with a high chance. In the context of the brute MCS, the coefficient of variation of the failure probability estimate P_f, denoted as δ_{Pf}, is approximated as follows (Ang and Tang 2007).

$$\delta_{Pf} \approx \sqrt{\frac{1-P_f}{n_{MCS} \cdot P_f}} \tag{8}$$

where n_{MCS} represents the number of samples utilized in the MCS. With the estimated failure probability P_f and its COV, the 90% confidence interval of the failure probability P_f shown in Figure 5(c) can readily be obtained with an assumption that the estimated failure probability follows a lognormal distribution. From there, the accuracy of the adopted SSM in evaluating the design robustness and safety of the reinforced slope is validated. However, with the SSM, only 390 realizations (or samples) of the uncertain input parameters are required. As such, the computational efficiency of the proposed optimization design could be guaranteed.

Since a discrete design space is adopted in this example, the design safety, robustness, and cost for each and every candidate design could be evaluated and the results are shown in Figure 6. The performance evaluation of these 480 candidate designs took approximately 30 days utilizing parallel computing on the Windows 7® PC equipped with a 192 GB RAM and an Intel® Xeon® Processor E5-2699 v4 @ 2.20 GHz. To be compatible with the conventional deterministic and probabilistic approaches, the design safety in this example is measured with the mean of the stability $E[FS_2]$ and the reliability index β (or equivalent failure probability P_f) of the reinforced slope, respectively. Figure 6(a) depicts the relationship between the mean of the stability $E[FS_2]$ and the cost C. Figure 6(b) depicts the relationship between the reliability index β and the cost C. Figure 6(c) depicts the relationship between the robustness R and the cost C. In Figure 6(a) and Figure 6(b), the design safety tends to increase with the increase of the cost C, as indicated by the increase of the mean of the stability $E[FS_2]$ and increase of the reliability index β. In Figure 6(c), the robustness also increases with the increase of the cost. Thus, a more conservative and robust design will cost more, indicating that a tradeoff exists between the safety (and robustness) and the cost. However, the various combinations of the design parameters means that the candidate designs of similar cost level may yield different levels of safety and robustness, and the candidate designs of different cost level may yield similar level of safety and robustness. Indeed, these combinations of the design parameters provide the theoretical basis for the optimization-based design of stabilizing piles.

In reference to the optimization algorithm of the stabilizing piles shown in Eq. (6), the design of the stabilizing piles in this example slope is readily undertaken. Through the sorting algorithm in the NSGA-II (Deb et al. 2002), a Pareto front consisting of nine non-dominated designs is established in the selected design space ***DS***, as depicted in Figure 6(c). This Pareto front shows the tradeoff between the robustness and the cost. As can be seen from Figure 6(c), these non-dominated designs on the Pareto front are superior to all others in the design space (either costs less or yields higher design robustness). Next, the knee point on this Pareto front, as depicted in Figure 6(c), is identified with the minimum distance approach outlined in Gong et al. (2016a). Here, this knee point could be taken as the most preferred design in the design space if the design constraint of the target stability ***TS*** is not applied.

It should be noted that the choice of the target stability ***TS*** can affect the resulting design, as indicated by the design results obtained with different choices of the target stability ***TS*** shown in Figure 7 and Table 4. The design results, in terms of the Pareto front and knee point, obtained with two different levels of target *FS* (i.e., FS_{T} = 1.20 and 1.25) (MCPRC 2002) are illustrated in Figure 7(a) and Figure 7(b). Similarly, the design results obtained with two different levels of target reliability index (i.e., β_T = 2.6 and 3.2) are shown in Figure 7(c) and Figure 7(d). The design results in Figure 7 and Table 4 depict that a reduction in the target stability ***TS***, as reflected by the decrease of target factor of safety and the decrease of target reliability index, could result in more feasible designs and more non-dominated designs (on the Pareto front); and, the associated most preferred design, in terms of the knee point on the Pareto front, will generally yield a smaller cost (desirable) and lower safety (not desirable), even though the most preferred design derived with $\beta_T = 2.6$ and that derived with $\beta_T = 3.2$ are identical in this problem. The design results that two different target reliability indexes yield the same knee point design might be caused by the parameters setting of the design space. The advantages of the Pareto front and knee point for identifying the most preferred design of the stabilizing piles, as presented in this paper, are not fully realized because of the finite number of candidate designs. For example, only three possible values of pile diameter are available. As a matter of fact, the Pareto fronts derived in the multi-objective optimizations are often continuous curves; whereas, the Pareto fronts derived in this example are contiguous polylines, as shown in Figure 7. Thus, the Pareto fronts shown in Figure 7 may not reveal the theoretical (or mathematical) tradeoff between the robustness and the cost in the design of the stabilizing piles, but only the tradeoff between the robustness and the cost in the design space analyzed. Similarly, the knee points shown in Figure 7 and Table 4 may only indicate the most preferred designs in the design space. However, the discrete design space adopted in this study could be deemed rational and acceptable owing to the following reasons: 1) some design parameters of the stabilizing piles could only be taken as discrete values (due to equipment or local practice); and 2) computational efficiency issue would not allow for the numerical analysis of an infinite number of candidate designs.

3.3 Comparison between advanced design framework and conventional designs

The conventional geotechnical design approaches (either deterministic or probabilistic) tend to focus on the design safety; thus, the design of stabilizing piles with such approaches can be implemented as a single-objective optimization problem: the design constraints are the design space ***DS*** and target stability ***TS***, and the objective is to minimize the cost C. With this single-objective optimization algorithm, the stabilizing piles in this slope are designed and the design results are compared here to those obtained from the advanced design framework.

As mentioned above, a conservative estimate of the uncertain input parameters and a target factor of safety FS_T are usually taken in the deterministic design approach to overcome the uncertainty involved. The following design scenarios are studied for comparison purposes: the conservative estimate of the soil strength parameters is simulated by taking the 50th, 40th and 30th percentiles of the assumed distributions (see Table 1), and the target factor of safety FS_T is taken as 1.20. The designs obtained with all these design scenarios are given in Table 5. The data in Table 5 depict that a more conservative estimate of the uncertain input parameters could lead to a more conservative and costly design. However, the true safety or the degree of conservativeness of the design is not known. Thus, the resulting design may be either over- or under-designed depending upon the degree of conservativeness adopted (in the estimation of the uncertain input parameters and the selection of target factor of safety FS_T). For example, if the 40th percentiles of the assumed distributions are taken as the inputs, the resulting design is fairly conservative in this problem (i.e., the reliability index β is close to 4.0 and the failure probability P_f is 3.61×10^{-5}). Further, if the 30th percentiles of the assumed distributions are taken, no feasible designs can be identified in the design space ***DS*** shown in Table 2.

Next, the stabilizing piles in this slope are designed utilizing the probabilistic approach. With the relationship between the reliability index β and the cost C illustrated in Figure 6(b), the least cost design that is above the target reliability index β_T can be located and taken as the most preferred design. For comparison purposes, the following two levels of target reliability index β_T are studied: β_T = 2.6 and 3.2. The designs obtained from these two target reliability indexes are tabulated in Table 5. The results indicate that a more conservative target reliability index could lead to a more conservative and costly design. Since the uncertainty in the input parameters can be explicitly considered, the *true* safety of the design, in terms of the failure probability P_f, is known to the engineer, which allows for a more informed design decision. However, the statistical information of the input geotechnical parameters, a prerequisite for the probabilistic designs, is often difficult to estimate with certainty due to limited availability of site-specific data. Thus, the effectiveness of the probabilistic design can be degraded by the inaccurate statistical characterization of the input geotechnical parameters (Juang and Wang 2013; Wang et al. 2013).

With the design results presented above, a comparison between the designs obtained with the conventional design approaches and those obtained with the advanced design framework is made, as shown in Figure 8. This comparison focuses on the cost C, design safety (in terms of the failure probability P_f) and design robustness R. The comparison between the deterministic approach and the advanced framework is shown in Figure 8(a), and the comparison between the probabilistic approach and the advanced framework is shown in Figure 8(b). It can be seen from Figure 8 that the robustness of the designs derived from the advanced design framework is always greater than that of the designs obtained from the conventional design approaches. Figure 8(a) shows that when the 50th percentiles of the assumed distributions are taken as the inputs, the deterministic design approach results in a 33% reduction in the cost while increasing the failure probability by 4.8 times, which is not desirable; and, when the 40th percentiles of the assumed distributions are taken, the deterministic approach results in a 100% increase in the cost and the associated failure probability is reduced to 3.61×10^{-5}, which appears to be overly conservative. Thus, the designs derived from the deterministic approach might be either cost-inefficient or overly conservative, when the uncertainty is present but not explicitly included. In Figure 8(b), when the target reliability index β_T, in the probabilistic approach, is taken as 2.6, the probabilistic approach leads to a 43% reduction in the cost while the failure probability is increased 6.6 times, which is not desirable; and, when the target reliability index β_T is taken as 3.2, the cost and the failure probability of the design obtained from the probabilistic approach are reduced 29% and 25%, respectively. That is to say, the advantages of the advanced design framework over the probabilistic approach are not evident when the target reliability index β_T is taken as 3.2, which could be attributed to the fact that the target reliability index of β_T = 2.6 and that of β_T = 3.2 yield the same knee point design (because of the discrete design space adopted), as shown in Figure 7(c) and Figure 7(d).

Limited availability of site-specific data, in a typical geotechnical practice, can hinder an accurate characterization of the statistics of input geotechnical parameters. In general, the autocorrelation structure is the most difficult to characterize, the COV less so, and the mean the easiest (Gong et al. 2017). A parametric study is undertaken to study the influences of the COV and vertical scale of fluctuation (which describes the vertical autocorrelation structure) on the variation of the stability of reinforced slope. For illustration purposes, the study results of the preferred designs listed in Table 4 and Table 5 are shown in Figure 9 and Figure 10. As can be seen, although the variation of the stability of reinforced slope are greatly influenced by the input statistics (of geotechnical parameters), the influence on the designs obtained with the advanced design framework is less significant; and, the design obtained with the advanced framework tends to yield a smaller variation of the stability of the reinforced slope. In other words, the performances of the designs obtained with the advanced design framework tend to be more robust against, or insensitive to, the uncertainty in the statistical characterization of the input geotechnical parameters. Hence, the superiority of the advanced design framework over the conventional design approaches in the aspect of design robustness is demonstrated.

4. Concluding Remarks

This paper presents a new optimization-based design framework for stabilizing piles. The advanced design framework consists of three components: 1) the coupling between the stabilizing piles and the slope, which is explicitly modeled with the finite difference program; 2) the spatial variability of the input geotechnical parameters, which is characterized with the random field theory, and its influence on the design of stabilizing piles is evaluated with the formulated design robustness; and 3) the optimization-based design, which is implemented as a multi-objective optimization considering the design robustness, economic aspect and safety requirements. This optimization-based design will only lead to a Pareto front, indicating the tradeoff between robustness and cost among all designs that can satisfy the design constraints (primarily safety). This Pareto front can aid in the informed design decision making process. For example, the knee point on this Pareto front that yields the best compromise with respect to the conflicting design objectives may be taken as the most preferred (or final) design.

The effectiveness of the advanced framework is demonstrated through an illustrative example, the design of stabilizing piles in a homogeneous earth slope. It should be noted that apart from the spatial variability of the input geotechnical parameters, both model uncertainty and structural parameters uncertainty are also explicitly included in this example. The results indicate that this new framework can be compatible with the conventional design approaches.

The comparison between the designs obtained with the advanced framework and those obtained with the conventional design approaches indicate that while the former might cost more, the benefit in the improvement of the design safety is much more significant. Further, the designs obtained with the advanced design framework are more robust against, or insensitive to, the uncertainty in the statistical characterization of the geotechnical parameters. Since the advanced design framework is built upon the foundation of conventional design approaches (either deterministic or probabilistic) by considering explicitly an additional design objective, namely, the design robustness, the advanced framework could be seen as a complementary design strategy to the existing design approaches.

It is noted that the optimization of stabilizing piles is a challenging problem, especially in the face of uncertainty. While the advanced design framework can be deemed effective, the following limitations will warrant further investigation: 1) the computational efficiency of the analysis and optimization of stabilizing piles caused by the coupling of numerical analysis and random field modeling; 2) the advantages of the Pareto front and knee point for identifying the most preferred design are not fully realized due to the discrete design space adopted; and 3) the behavior of the pile-slope system is much more complicated than that derived from the 2-D numerical analysis. Nevertheless, the design framework advanced could be regarded as a significant step towards an improved design of stabilizing piles in the face of uncertainty.

Acknowledgments

The financial support provided by the National Natural Science Foundation of China (No. 41702294 and No. 41977242) and the National Key R&D Program of China (No. 2017YFC1501302) is acknowledged. The fourth author would also like to acknowledge the support by the National Science Foundation through Grant HRD-1818649. The results and opinions expressed in this paper do not necessarily reflect the views and policies of both the National Natural Science Foundation of China and the National Science Foundation.

References

Ang, A.H.S., and Tang, W.H. (2007). Probability Concepts in Engineering: Emphasis on Application to Civil and Environmental Engineering (2nd Ed.), Wiley, New York.

Beyer, H.G., and Sendhoff, B. (2007). Robust optimization - A comprehensive survey. Computer methods in applied mechanics and engineering, 196(33-34), 3190-3218.

Chen, C.Y., and Martin, G.R. (2002). Soil-structure interaction for landslide stabilizing piles. Computers and Geotechnics, 29(5), 363-386.

Cherubini, C. (2000). Reliability evaluation of shallow foundation bearing capacity on c', φ' soils. Canadian Geotechnical Journal, 37(1), 264-269.

Ching, J., and Phoon, K.K. (2013). Mobilized shear strength of spatially variable soils under simple stress states. Structural Safety, 41(3), 20-28.

Cho, S.E. (2007). Effects of spatial variability of soil properties on slope stability. Engineering Geology, 92(3), 97-109.

Christian, J.T., Ladd, C.C., and Baecher, G.B. (1994). Reliability applied to slope stability analysis. Journal of Geotechnical Engineering, 120(12), 2180-2207.

Comodromos, E.M., Papadopoulou, M.C., and Rentzeperis, I.K. (2009). Effect of cracking on the response of pile test under horizontal loading. Journal of Geotechnical and Geoenvironmental Engineering, 135(9), 1275-1284.

Dawson, E.M., Roth, W.H., and Drescher, A. (1999). Slope stability analysis by strength reduction. Géotechnique, 49(6), 835-840.

Deb, K., Pratap, A., Agarwal, S., and Meyarivan, T. (2002). A fast and elitist multi-objective genetic algorithm: NSGA-II. IEEE Transactions on Evolutionary Computation, 6(2), 182-197.

Deb, K., and Gupta, S. (2011). Understanding knee points in bicriteria problems and their implications as preferred solution principles. Engineering Optimization, 43(11), 1175-1204.

Duncan, J.M. (2000). Factors of safety and reliability in geotechnical engineering. Journal of Geotechnical and Geoenvironmental Engineering, 126(4), 307-316.

Fenton, G.A. (1999). Random field modeling of CPT data. Journal of Geotechnical and Geoenvironmental Engineering, 125(6), 486-498.

FLAC version 7.0. (2011). Fast Lagrangian Analysis of Continua, Minneapolis, USA: Itasca Consulting Group Inc.

Galli, A., and Di Prisco, C. (2012). Displacement-based design procedure for slope-stabilizing piles. Canadian Geotechnical Journal, 50(1), 41-53.

Gong, W., Wang, L., Juang, C.H., Zhang, J., and Huang, H. (2014a). Robust geotechnical design of shield-driven tunnels. Computers and Geotechnics, 56, 191-201.

Gong, W., Khoshnevisan, S., and Juang, C.H. (2014b). Gradient-based design robustness measure for robust geotechnical design. Canadian Geotechnical Journal, 51(11), 1331-1342.

Gong, W., Juang, C.H., Khoshnevisan, S., and Phoon, K.K. (2016a). R-LRFD: Load and resistance factor design considering robustness. Computers and Geotechnics, 74, 74-87.

Gong, W., Juang, C.H., Martin, J.R., and Ching, J. (2016b). New sampling method and procedures for estimating failure probability. Journal of Engineering Mechanics, 142(4), 04015107.

Gong, W., Tien, Y.M., Juang, C.H., Martin, J.R., and Luo, Z. (2017). Optimization of site investigation program for improved statistical characterization of geotechnical property based on random field theory. Bulletin of Engineering Geology and the Environment, 76(3), 1021-1035.

Griffiths, D.V., and Fenton, G.A. (2004). Probabilistic slope stability analysis by finite elements. Journal of Geotechnical and Geoenvironmental Engineering, 130(5), 507-518.

Hajela, P., and Lin, C.Y. (1992). Genetic search strategies in multicriterion optimal design. Structural Optimization, 4(2), 99-107.

Horn, J., Nafpliotis, N., and Goldberg, D.E. (1994). A niched Pareto genetic algorithm for multiobjective optimization. In Proceedings of the first IEEE conference on Evolutionary Computation, IEEE World Congress on Computational Intelligence, New York, 82-87.

Huang, Z.H., Zhang, L.L., Cheng, S. Y., Zhang, J., and Xia, X.H. (2014). Back-analysis and parameter identification for deep excavation based on Pareto multiobjective optimization. Journal of Aerospace Engineering, 28(6), A4014007.

Ito, T., and Matsui, T. (1975). Methods to estimate lateral force acting on stabilizing piles. Soils and Foundations, 15(4), 43-59.

Jeong, S., Kim, B., Won, J., and Lee, J. (2003). Uncoupled analysis of stabilizing piles in weathered slopes. Computers and Geotechnics, 30(8), 671-682.

Juang, C.H., and Wang, L. (2013). “Reliability-based robust geotechnical design of spread foundations using multi-objective genetic algorithm.” Computers and Geotechnics, 48, 96-106.

Juang, C.H., Wang, L., Hsieh, H.S., and Atamturktur, S. (2014). Robust geotechnical design of braced excavations in clays. Structural Safety, 49, 37-44.

Juang, C.H., Gong, W., and Martin, J.R. (2017). Subdomain sampling methods – Efficient algorithm for estimating failure probability. Structural Safety, 66, 62-73.

Juang, C.H., Gong, W., Martin II, J. R., and Chen, Q. (2018). Model selection in geological and geotechnical engineering in the face of uncertainty – Does a complex model always outperform a simple model? Engineering Geology, 242, 184-196.

Kawa, M., and Puła, W. (2019). 3D bearing capacity probabilistic analyses of footings on spatially variable c–φ soil. Acta Geotechnica, 1-14.

Khoshnevisan, S., Gong, W., Juang, C.H., and Atamturktur, S. (2014). Efficient robust geotechnical design of drilled shafts in clay using a spreadsheet. Journal of Geotechnical and Geoenvironmental Engineering, 141(2), 4014092.

Kourkoulis, R., Gelagoti, F., Anastasopoulos, I., and Gazetas, G. (2010). Slope stabilizing piles and pile-groups: parametric study and design insights. Journal of Geotechnical and Geoenvironmental Engineering, 137(7), 663-677.

Lee, C.Y., Hull, T.S., and Poulos, H.G. (1995). Simplified pile-slope stability analysis. Computers and Geotechnics, 17(1), 1-16.

Li, D.Q., Chen, Y., Lu, W., and Zhou, C. (2011). Stochastic response surface method for reliability analysis of rock slopes involving correlated non-normal variables. Computers and Geotechnics, 38(1), 58-68.

Li, D.Q., Jiang, S.H., Cao, Z.J., Zhou, W., Zhou, C.B., and Zhang, L.M. (2015). A multiple response-surface method for slope reliability analysis considering spatial variability of soil properties. Engineering Geology, 187, 60-72.

Li, D.Q., Xiao, T., Cao, Z.J., Zhou, C.B., and Zhang, L.M. (2016). Enhancement of random finite element method in reliability analysis and risk assessment of soil slopes using subset simulation. Landslides, 13(2), 293-303.

Li, D. Q., Yang, Z. Y., Cao, Z. J., Au, S. K., and Phoon, K. K. (2017). System reliability analysis of slope stability using generalized subset simulation. Applied Mathematical Modelling, 46, 650-664.

Li, K.S., and Lumb, P. (1987). Probabilistic design of slopes. Canadian Geotechnical Journal, 24(4), 520-535.

Lirer, S. (2012). Landslide stabilizing piles: Experimental evidences and numerical interpretation. Engineering Geology, 149, 70-77.

Liu, L. L., and Cheng, Y. M. (2018). System Reliability Analysis of Soil Slopes Using an Advanced Kriging Metamodel and Quasi–Monte Carlo Simulation. International Journal of Geomechanics, 18(8), 06018019.

Ministry of Construction of the People’s Republic of China (MCPRC) (2002). Technical Code for Building Slope Engineering (GB50330-2002). China Building Industry Press, Beijing (in Chinese).

Murata, T., and Ishibuchi, H. (1995). MOGA: Multi-objective genetic algorithms. In 1995 IEEE International Conference on Evolutionary Computation, New York, 289-294.

Phadke, M.S. (1989), Quality Engineering Using Robust Design, Prentice Hall. Englewood Cliffs, New Jersey.

Poulos, H.G. (1995). Design of reinforcing piles to increase slope stability. Canadian Geotechnical Journal, 32(5), 808-818.

Taguchi, G. (1986). Introduction to Quality Engineering: Designing Quality into Products and Processes, Quality Resources, White Plains, New York.

Tang, H., Hu, X., Xu, C., Li, C., Yong, R., and Wang, L. (2014). A novel approach for determining landslide pushing force based on landslide-pile interactions. Engineering Geology, 182, 15-24.

Tang, H., Wasowski, J., and Juang, C.H. (2019). Geohazards in the three Gorges Reservoir Area, China–Lessons learned from decades of research. Engineering Geology, 105267.

Tian, M., Li, D.Q., Cao, Z.J., Phoon, K.K., and Wang, Y. (2016). Bayesian identification of random field model using indirect test data. Engineering Geology, 210, 197-211.

Tun, Y. W., Llano-Serna, M. A., Pedroso, D. M., and Scheuermann, A. (2019). Multimodal reliability analysis of 3D slopes with a genetic algorithm. Acta Geotechnica, 14(1), 207-223.

Vrugt, J.A., and Robinson, B.A. (2007). Improved evolutionary optimization from genetically adaptive multimethod search. Proceedings of the National Academy of Sciences, 104(3), 708-711.

Wang, L., Hwang, J.H., Juang, C.H., and Atamturktur, S. (2013). Reliability-based design of rock slopes – A new perspective on design robustness. Engineering Geology, 154, 56-63.

Wang, F., Li, H., and Zhang, Q. L. (2017). Response–Surface–Based Embankment Reliability under Incomplete Probability Information. International Journal of Geomechanics, 17(12), 06017021.

Wang, X., Wang, H., and Liang, R.Y. (2018). A method for slope stability analysis considering subsurface stratigraphic uncertainty. Landslides, 15(5), 925-936.

Wang, Y., Cao, Z., and Au, S. K. (2010). Efficient Monte Carlo simulation of parameter sensitivity in probabilistic slope stability analysis. Computers and Geotechnics, 37(7-8), 1015-1022.

Wiśniewski, D.F., Cruz, P.J., Henriques, A.A.R., and Simões, R.A. (2012). Probabilistic models for mechanical properties of concrete, reinforcing steel and pre-stressing steel. Structure and Infrastructure Engineering, 8(2), 111-123.

Xiao, T., Li, D. Q., Cao, Z. J., Au, S. K., and Phoon, K. K. (2016). Three-dimensional slope reliability and risk assessment using auxiliary random finite element method. Computers and Geotechnics, 79, 146-158.

Xiao, T., Li, D. Q., Cao, Z. J., and Tang, X. S. (2017). Full probabilistic design of slopes in spatially variable soils using simplified reliability analysis method. Georisk: Assessment and Management of Risk for Engineered Systems and Geohazards, 11(1), 146-159.

Zeng, S., and Liang, R.Y. (2002). Stability analysis of drilled shafts reinforced slope. Soils and Foundations, 42(2), 93-102.

Zhang, J., Wang, H., Huang, H. W., and Chen, L. H. (2017). System reliability analysis of soil slopes stabilized with piles. Engineering Geology, 229, 45-52.

Zhao, Y.G., and Ono, T. (2001). Moment methods for structural reliability. Structural Safety, 23(1), 47-75.

Appendix A. Subdomain Sampling Method (SSM) for Estimating the Statistics of System Behavior

The essence of the SSM is to partition the possible domain of uncertain variables into a set of subdomains and then to generate samples of uncertain variables in each and every subdomain separately (Juang et al., 2017). In which, a distance index (d) based upon Hasofer-Lind reliability index is adopted to locate the possible domain and to partition this domain.

$$d = \sqrt{[\boldsymbol{n}]^{\mathrm{T}} [\boldsymbol{R}_{\boldsymbol{n}}]^{-1} [\boldsymbol{n}]} \tag{A1}$$

where $\boldsymbol{R}_{\boldsymbol{n}}$ is the correlation matrix among the equivalent standard normal variables $\boldsymbol{n} = [n_1, n_2, \ldots, n_{n_x}]^{\mathrm{T}}$, where n_x is the number of uncertain variables. The standard normal variable n_i in $\boldsymbol{n}$ is related to the uncertain variable x_i in $\boldsymbol{x}$.

$$n_i = \Phi^{-1}[F(x_i)] \tag{A2}$$

where $F(x_i)$ is the cumulative distribution function (CDF) of uncertain variable x_i, and $\Phi(\cdot)$ is the CDF of the standard normal variable. With the distance index formulated in Eq. (A1), the possible domain of uncertain variables $\boldsymbol{x}$, denoted as $[0, d_{\max})$, can be located.

$$\chi^2_{n_x}(d^2_{\max}) = \varepsilon \tag{A3}$$

where $\chi^2_{n_x}(\cdot)$ is the chi-square CDF with n_x degrees of freedom, and ε is a probability which is relatively low. The located possible domain of uncertain variables $\boldsymbol{x}$, in terms of $[0, d_{\max})$, is readily partitioned into a set of subdomains, in terms of $[d_0, d_1)$, $[d_1, d_2)$, $[d_2, d_3)$, etc. The likelihoods of the uncertain variables $\boldsymbol{x}$ being located in these subdomains could be taken as a decreasing sequence for the purpose of being computationally efficient.

$$p_{di} = \Pr\left[d_{i-1} \le \sqrt{[\boldsymbol{n}]^{\mathrm{T}} [\boldsymbol{R}]^{-1} [\boldsymbol{n}]} < d_i \right] = \Pr\left[d_{i-1}^2 \le d^2 < d_i^2 \right] = \chi_{n_x}^2 (d_i^2) - \chi_{n_x}^2 (d_{i-1}^2) \quad \text{(A4)}$$

where p_{di} is the likelihood of the uncertain variables $\boldsymbol{x}$ being located in the subdomain $[d_{i-1}, d_i)$. Then, the samples of uncertain variables $\boldsymbol{x}$ are generated in each subdomain. The procedures for generating a target number of samples in the subdomain $[d_{i-1}, d_i)$ are given in Gong et al. (2016b).

For ease of programing, a same target number of samples, denoted as t_1, is adopted in all these subdomains and this target number is taken as: $t_1 = 10p_{di}/p_{d(i-1)}$. With the generated samples of uncertain variables, the deterministic analysis of the system behavior can readily be undertaken, from which the statistics of the system behavior, in terms of the mean $E[g]$, the standard deviation $\sigma[g]$, the skewness α_3[g] and the kurtosis α_4[g], can be approximated as:

$$E[g] \approx \sum_{i=1}^{i=n_s} \sum_{j=1}^{j=t_1} p_{ij} \cdot g_{ij} \quad \text{(A5)}$$

$$\sigma[g] \approx \left[\sum_{i=1}^{i=n_s} \sum_{j=1}^{j=t_1} p_{ij} \cdot \left(g_{ij} - E[g] \right)^2 \right]^{0.5} \quad \text{(A6)}$$

$$\alpha_3[g] \approx \sum_{i=1}^{i=n_s} \sum_{j=1}^{j=t_1} p_{ij} \cdot \left(\frac{g_{ij} - E[g]}{\sigma[g]} \right)^3 \quad \text{(A7)}$$

$$\alpha_4[g] \approx \sum_{i=1}^{i=n_s} \sum_{j=1}^{j=t_1} p_{ij} \cdot \left(\frac{g_{ij} - E[g]}{\sigma[g]} \right)^4 \quad \text{(A8)}$$

where g_{ij} is the system behavior evaluated with the jth sample in the ith subdomain, denoted as $\boldsymbol{x}_{ij}$; n_s is the number of subdomains; and, p_{ij} is the likelihood or probability of the sample $\boldsymbol{x}_{ij}$ being generated in the domain of uncertain variables, which could be expressed as:

$$p_{ij} = \frac{p_{di}}{t_1} = \frac{\chi_{n_x}^2 (d_i^2) - \chi_{n_x}^2 (d_{i-1}^2)}{t_1} \quad \text{(A9)}$$

List of Figures

List of Tables

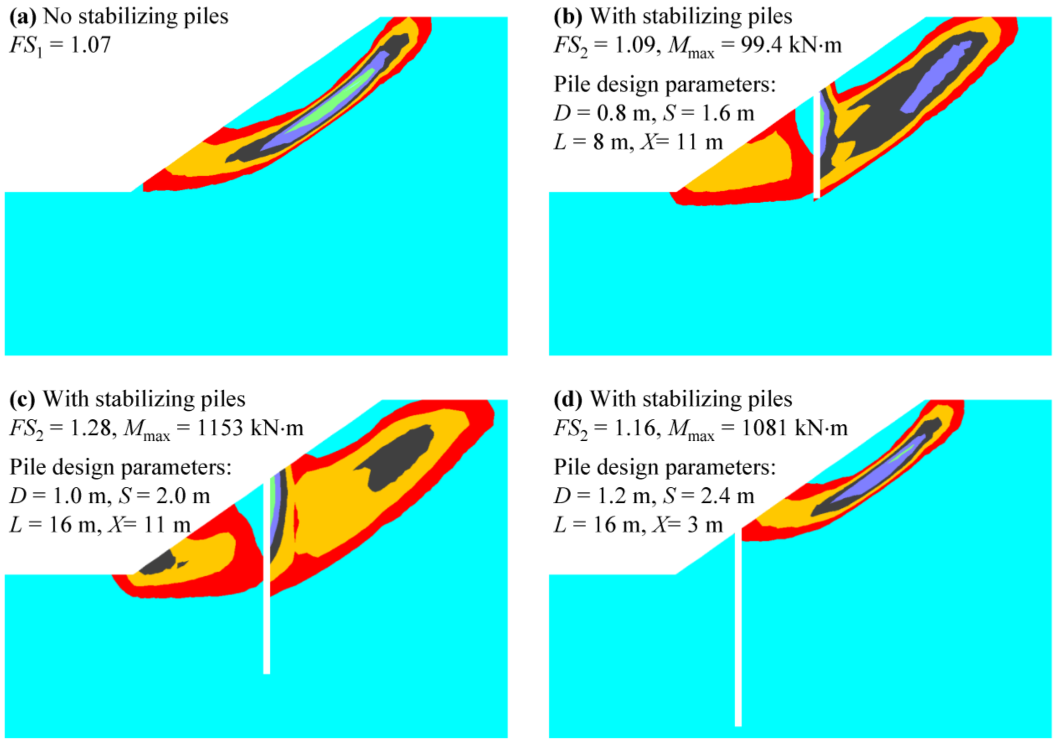

Figure 1. Conceptual illustration of the coupled behavior in the pile-slope system (notation: D is the pile diameter, S is the pile spacing in the longitudinal direction, L is the pile length, X is the pile location, FS_1 is the factor of safety of the unreinforced slope, FS_2 is the factor of safety of the reinforced slope, and M_{max} is the maximum bending moment of the piles)

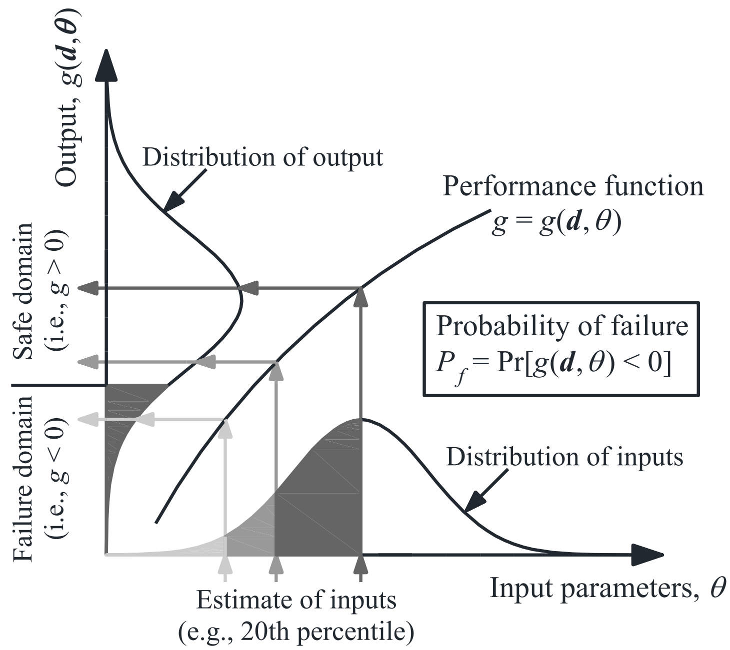

Figure 2. Conceptual illustration of the design under the influence of uncertainties

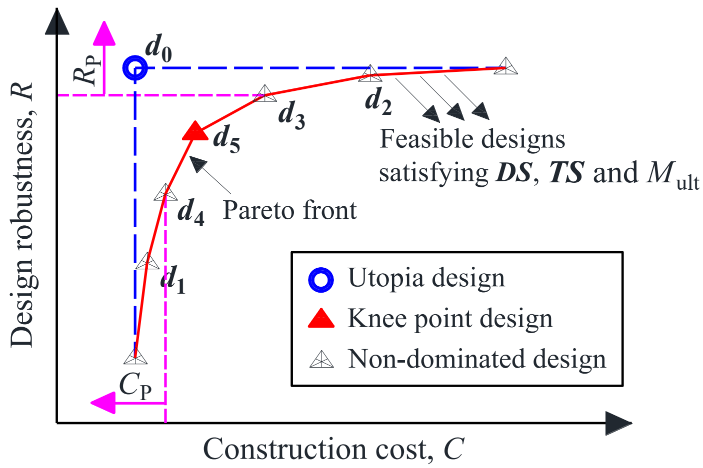

Figure 3. Conceptual illustration of the optimization results of stabilizing piles

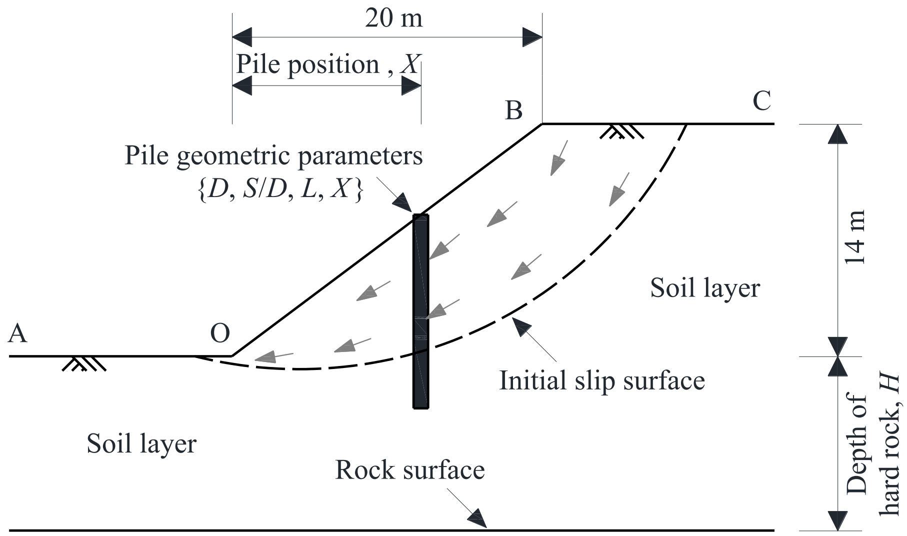

Figure 4. Schematic diagram of the illustrative example

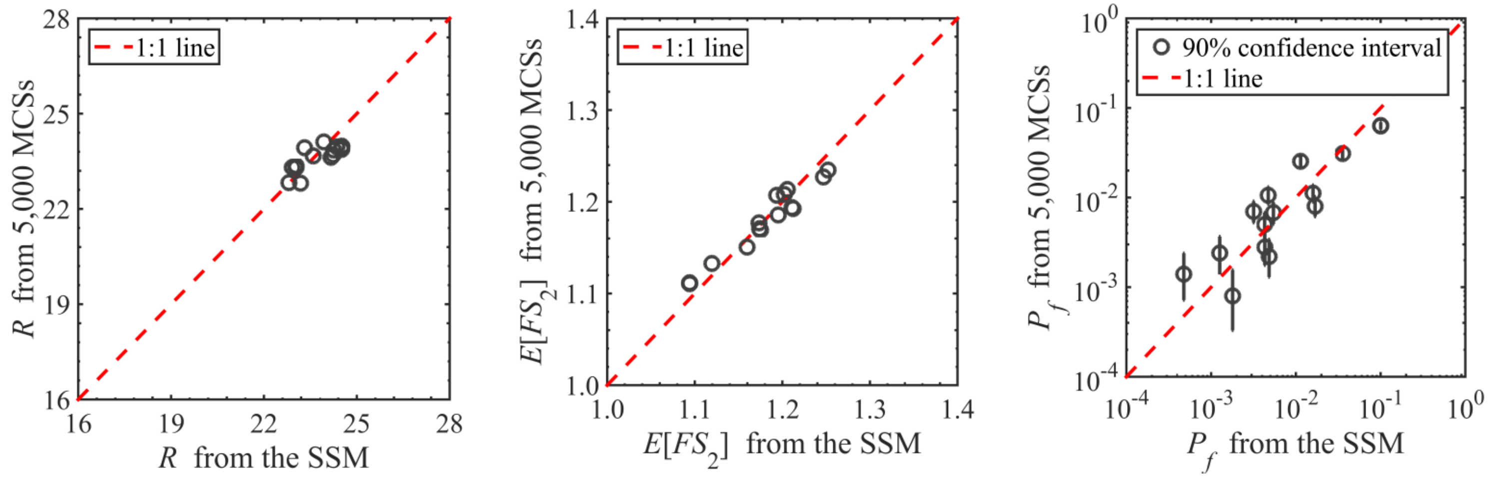

(a) Design robustness R **(b)** Design safety $E[FS_2]$ **(c)** Design safety P_f

Figure 5. Effectiveness of the adopted SSM in deriving the design robustness and safety

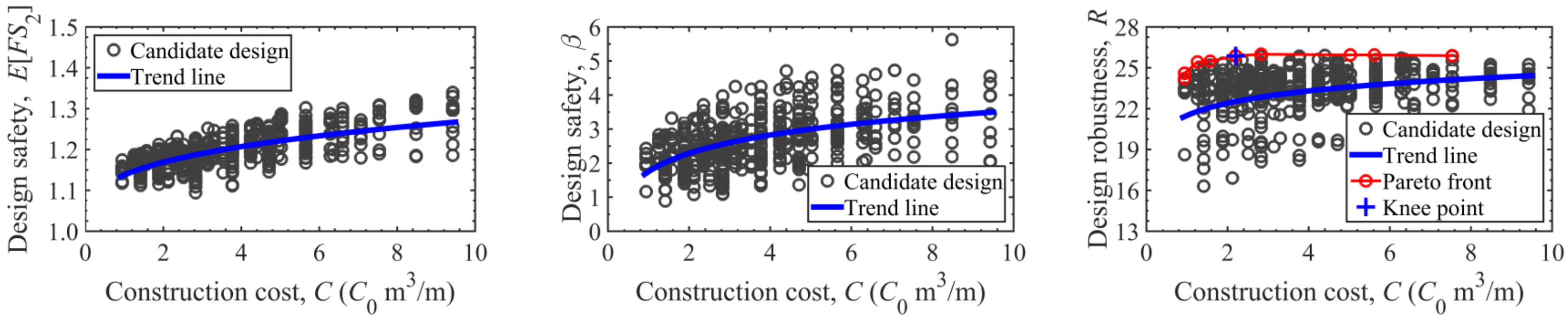

(a) Design safety $E[FS_2]$versus cost C **(b)** Design safety P_f versus cost C **(c)** Design robustness R versus cost C

Figure 6. Evaluation of the design safety, design robustness and construction cost for candidate designs in the design space ***DS***

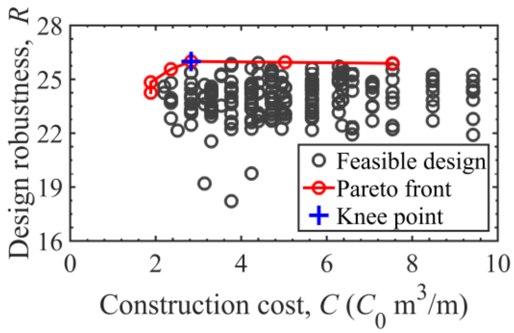

(a) Target stability ***TS*** of FS_{T} = 1.20

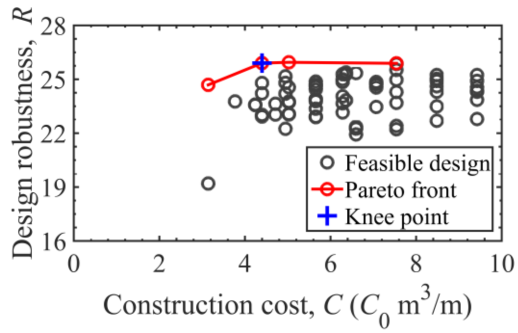

(b) Target stability ***TS*** of FS_{T} = 1.25

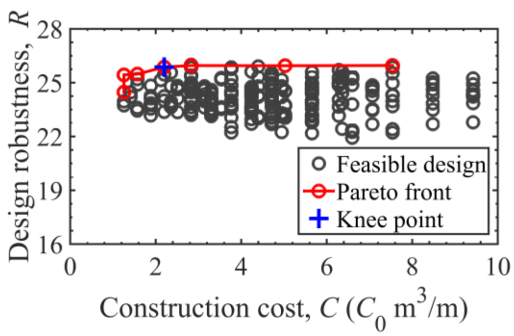

(c) Target stability ***TS*** of β_T = 2.6

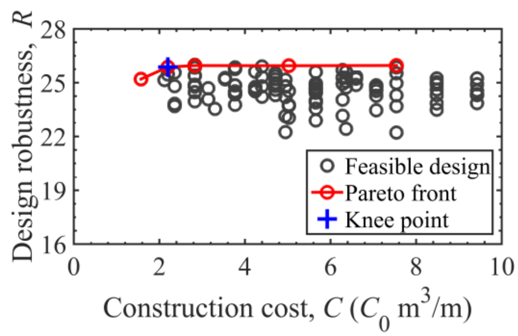

(d) Target stability ***TS*** of β_T = 3.2

Figure 7. Influence of the target stability ***TS*** on the design results of the stabilizing piles

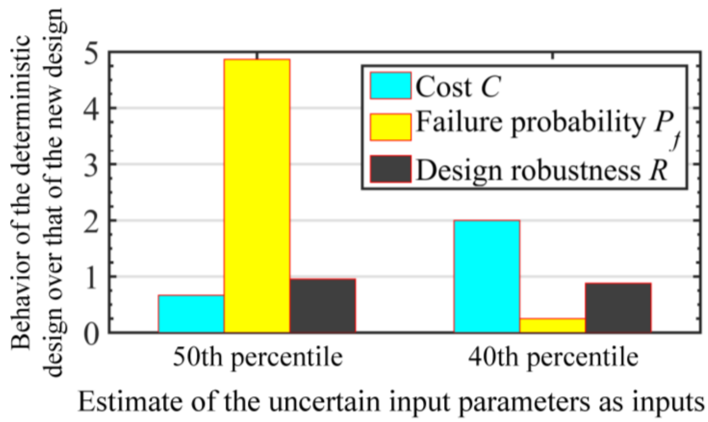

(a) Designs obtained with deterministic approach versus those with advanced framework (target stability ***TS*** is set up as $FS_T = 1.20$)

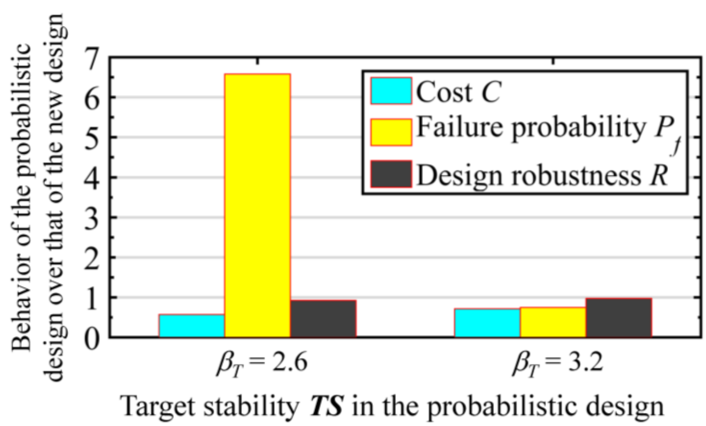

(b) Designs obtained with probabilistic approach versus those with advanced framework

Figure 8. Designs obtained with conventional design approaches versus those with the advanced design framework (Note: the vertical coordinate represents the ratio of the design objective of the designs obtained with the conventional design approaches over that of the designs obtained with advanced design framework)

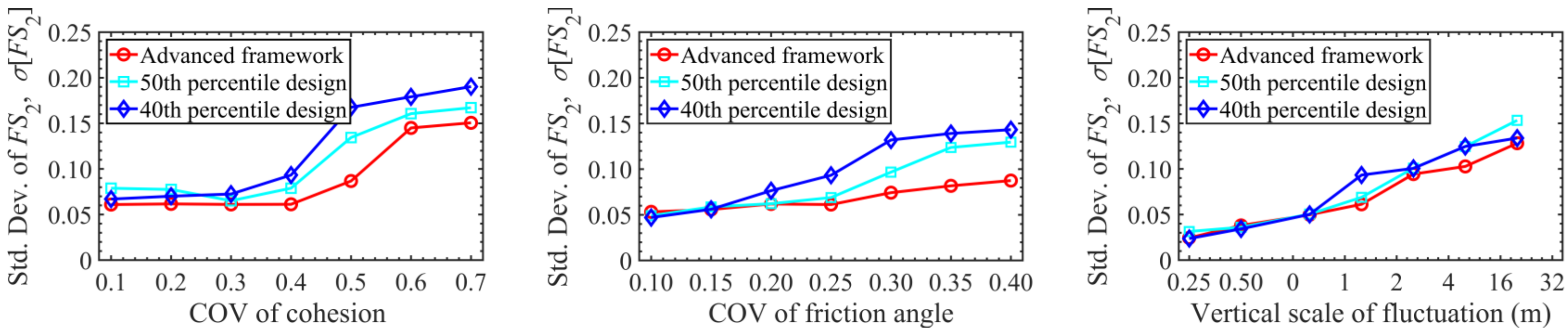

(a) COV of cohesion **(b)** COV of friction angle (c) Vertical scale of fluctuation

Figure 9. Influence of the input statistical information of soil strength parameters on the variation of the stability of reinforced slope (advanced framework versus deterministic approach: target stability FS_T = 1.20 and different percentiles of the inputs are taken)

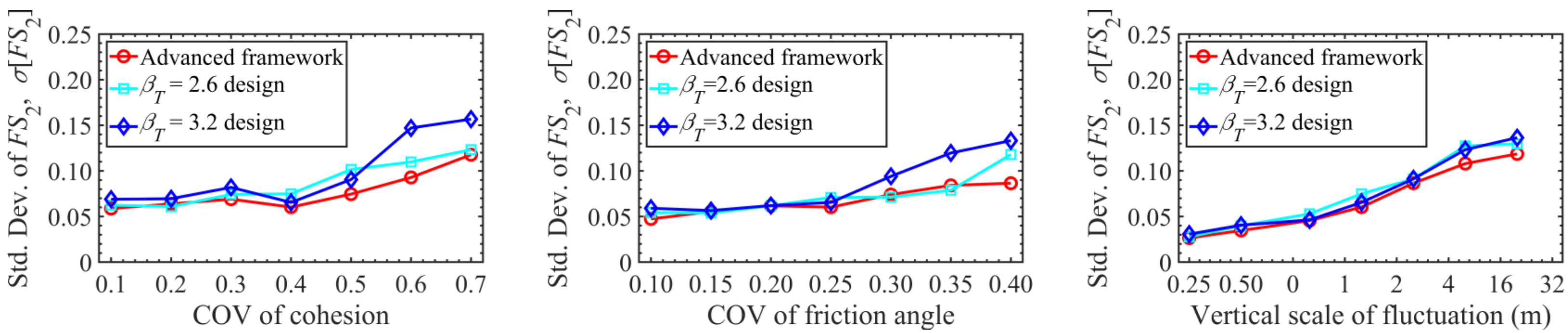

(a) COV of cohesion **(b)** COV of friction angle (c) Vertical scale of fluctuation

Figure 10. Influence of the input statistical information of soil strength parameters on the variation of the stability of reinforced slope (advanced framework versus probabilistic approach: different target reliability index β_T are studied)

Table 1. Statistical information of the uncertain input parameters (or noise factors) in the illustrative example

Uncertain input parameters		Distribution	Mean	COV	Scale of fluctuation	
					Horizontal, λ_h	Vertical, λ_v
Soil strength parameters [a]	Cohesion, c	Lognormal	12.0 kPa	0.40 [b]	50.0 m	2.5 m
	Friction angle, ϕ	Lognormal	20.0 °	0.25 [b]	50.0 m	2.5 m
Structural properties	Yielding strength of steel bar	Normal	345×10^3 kPa	0.05 [c]	-	-
	Compression strength of concrete	Normal	39×10^3 kPa	0.12 [c]	-	-
Model error	(true *FS*) – (calculated *FS*)	Uniform	The distribution range is [-0.02, 0.02]			

Note: [a] the correlation coefficient between soil cohesion and soil friction angle is -0.5;
b data are from Cherubini (2000);
c data are from Wiśniewski et al. (2012).

Table 2. Deterministic parameters in the illustrative example

Category	Parameter	Value
Soil	Unit weight (kN/m^3)	17.0
	Bulk modulus (MPa)	330
	Shear modulus (MPa)	150
Stabilizing piles	Unit weight (kN/m^3)	25.0
	Young's modulus (GPa)	35.0
	Steel reinforcement ratio (%)	1.0
	Thickness of concrete protective cover (m)	0.05
Soil-pile interfaces	Normal stiffness (MPa/m)	550
	Shear stiffness (MPa/m)	550
	Cohesion (kPa)	12.0
	Friction angle (°)	20.0

Table 3. Design space ***DS*** selected in the illustrative example

Design parameters	Design pool (i.e., potential values of pile parameters)
Pile diameter, D (m)	{0.6 m, 0.9 m, 1.2 m}
Pile spacing, S (m)	$\{S \mid S/D = 2.0, S/D = 3.0\}$
Pile length, L (m)	{6 m, 8 m, 10 m, 12 m, 14 m, 16 m, 18 m, 20 m}
Pile position, X (m)	{1 m, 3 m, 5 m, 7 m, 9 m, 11 m, 13 m, 15 m, 17 m, 19 m}

Table 4. Optimal designs of the stabilizing piles obtained with the advanced design framework

Target stability ***TS***		Number of feasible designs	Number of non-dominated designs	Most preferred design							
				Pile design parameters ***d***				Cost, C (C_0 m^3/m)	Design safety		Design robustness, R
				D (m)	S (m)	L (m)	X (m)		$E[FS_2]$	β	
Factor of safety	$FS_T = 1.20$	217	6	0.9	2.7	12.0	5.0	2.827	1.22	3.624	25.995
	$FS_T = 1.25$	74	4	1.2	3.6	14.0	3.0	4.398	1.25	4.707	25.902
Reliability index	$\beta_T = 2.6$	256	7	0.6	1.8	14.0	5.0	2.199	1.19	3.237	25.870
	$\beta_T = 3.2$	111	5	0.6	1.8	14.0	5.0	2.199	1.19	3.237	25.870

Table 5. Optimal designs of the stabilizing piles obtained with the conventional geotechnical design approaches

Design approach		Pile design parameters ***d***				Cost, C (C_0 m^3/m)	Design safety			Design robustness, R
		D (m)	S (m)	L (m)	X (m)		$E[FS_2]$	β	P_f	
Deterministic approach (FS_T = 1.2)	50th percentile	0.9	2.7	8.0	3.0	1.885	1.20	3.192	7.06×10^{-4}	24.834
	40th percentile	1.2	2.4	12.0	5.0	5.655	1.30	3.969	3.61×10^{-5}	22.896
	30th percentile	The maximum FS_2 of the candidate pile design is less than FS_T = 1.2, and no feasible designs could be identified in the design space ***DS*** shown in Table 2.								
Probabilistic approach	β_T = 2.6	0.6	1.8	8.0	3.0	1.257	1.18	2.655	3.97×10^{-3}	23.953
	β_T = 3.2	0.6	1.8	10.0	5.0	1.571	1.19	3.320	4.51×10^{-4}	25.201